Mon. Not. R. astr. Soc. (1970) **149**, 221–235.

ON THE INTERACTION OF COSMIC X-RAYS WITH INTERSTELLAR GRAINS

P. G. Martin

(Communicated by D. W. Sciama)

(Received 1970 March 16)

SUMMARY

An investigation of the interaction of cosmic X-rays with interstellar grains has been undertaken to determine what might be learned about the grains by observations at X-ray energies. To begin, a review of the extinction of X-rays by grains is given. Then the phenomenon of the X-ray halo is discussed. The many factors which can affect the intensity distribution of the halo are stressed so that in interpreting the observations a good estimate of the grain size and shape can be made.

X-ray observations may be useful in identifying light elements in grains. Near the K edge of an element in a grain the scattering is anomalous. The resulting effect on the intensity of the halo is shown to be appreciable in favourable cases. There is also a characteristic fine structure in the K absorption by elements in a solid. Estimates indicate that with large enough optical depths the presence of the lighter elements might be detectable.

1. INTRODUCTION

In this paper the interaction of X-rays with interstellar grains is investigated in order to point out what may be learned about the grains from observations at X-ray energies. In Section 2 the theoretical basis of X-ray extinction by interstellar grains is reviewed to provide a reference for later applications. Following this is a discussion of the phenomenon of the X-ray halo, in which the importance of the many factors affecting the size and intensity distribution is stressed. An attempt is made to treat each individually. In the last sections some possibilities for the chemical identification of grains by X-ray techniques are assessed. The first is based on the characteristic change in the intensity of the halo (scattered radiation) as a result of anomalous dispersion near a K edge, whereas the second requires the observation of fine structure in the K absorption edges.

2. THE EXTINCTION OF X-RAYS BY GRAINS

Our description of the extinction of X-rays by grains will emphasize the phenomena involved rather than the mathematical detail which appears elsewhere (e.g. van de Hulst 1957). We begin by examining several overriding factors which are fundamental to the theory. One is the quantity $x = 2\pi a/\lambda$ which for wavelengths $\lambda < 50$ Å and grain sizes $a > 10^{-6}$ cm is much larger than one. One consequence of this that we shall use is that a ray may be traced through the grain. Next, for X-ray energies the complex refractive index of the grain

$$m(m = 1 - \delta - i\beta)$$

differs only slightly from one so that $|m-1| \ll 1$. As a result reflection and refraction are negligible. However, the most important factor is $\xi^* = 2x(m-1)$, the complex phase shift across the grain. Note that the asterisk does not denote a complex conjugate. The nature of the extinction is determined by the size of $|\xi^*|$.

The extinction may be divided into two parts, true absorption and scattering. The computation of the true absorption is straightforward. The imaginary part of $m(\beta)$ is related to the mass absorption coefficient γ by $\rho\gamma = 4\pi\beta/\lambda$, where ρ is the density of the material. A more fundamental relationship to the atomic photoelectric absorption coefficient σ is found through $\gamma = N\langle\sigma/M\rangle$ where N is Avogadro's number and M is the mass number, the brackets indicating an average over all the elements in the material. A ray of unit intensity passing through the grain emerges with intensity $\exp[-\gamma\rho p(\zeta, \eta)]$ where $p(\zeta, \eta)$ is the path length through the grain specified with rectangular co-ordinates ζ and η in a reference plane P behind the grain. Since an amount $1-e^{-\gamma\rho p}$ is absorbed the efficiency factor for absorption* is

$$Q_a = \iint_G (1-e^{-\gamma\rho p})\, d\zeta\, d\eta/G$$

where G is the area of the geometrical shadow in the plane P. When the grain is optically thin ($\gamma\rho p \ll 1$) the total absorption is the same as that from an equivalent number of atoms in the gaseous state. However, when the grain becomes optically thick the absorption saturates ($Q_a \to 1$) and the absorption is less than that from the equivalent gaseous state (Fig. 1).

A similar approach can be taken to describe the scattering. In the plane P behind the grain the amplitude of the field within the geometrical shadow is

$$\exp\left[-i\frac{2\pi}{\lambda}(m-1)\,p(\zeta, \eta)\right]$$

relative to a field of unity outside. According to Babinet's principle the field that has been added to the incident field (i.e. the scattered wave) is

$$\exp\left[-i\frac{2\pi}{\lambda}(m-1)\,p\right]-1.$$

An application of the Huygens–Fresnel principle then gives the amplitude function

$$S(\theta, \varphi) = \frac{1}{2\pi}\left(\frac{2\pi}{\lambda}\right)^2 \iint_G \left\{1-\exp\left[-i\frac{2\pi}{\lambda}(m-1)\,p\right]\right\} \times \exp\left[-i\frac{2\pi}{\lambda}(\zeta\cos\varphi+\eta\sin\varphi)\,\theta\right] d\zeta\, d\eta$$

where θ is the scattering angle ($\theta = 0$ in the forward direction) and φ is the azimuthal angle of the direction of the scattered wave. Only the linear terms have been retained in the second exponential factor. This is a Fraunhofer diffraction phenomenon with a non-uniformly illuminated aperture.

* The cross-section for extinction, C_e, is defined as the area which intercepts an amount of the incident radiation equal to the amount 'extinguished' by the grain, and the efficiency factor Q_e is the ratio C_e/G. The separate contributions of absorption and scattering are denoted by subscripts a and s respectively.

Several useful observations can be made without evaluating the integral for specific cases. First, the radiation is concentrated in a narrow cone about the forward direction because the aperture is much larger than the wavelength. When θ is large the second factor in the integrand oscillates rapidly, the net amplitude being very small. Similar considerations show that the cone is more extended in the directions in which the aperture is small. This is of interest to the halo phenomenon discussed in the next section. Second, when β is sufficiently large the grain is opaque; the remaining term in the curly brackets gives rise to the classical Fraunhofer diffraction (cFd). In this case the angular distribution

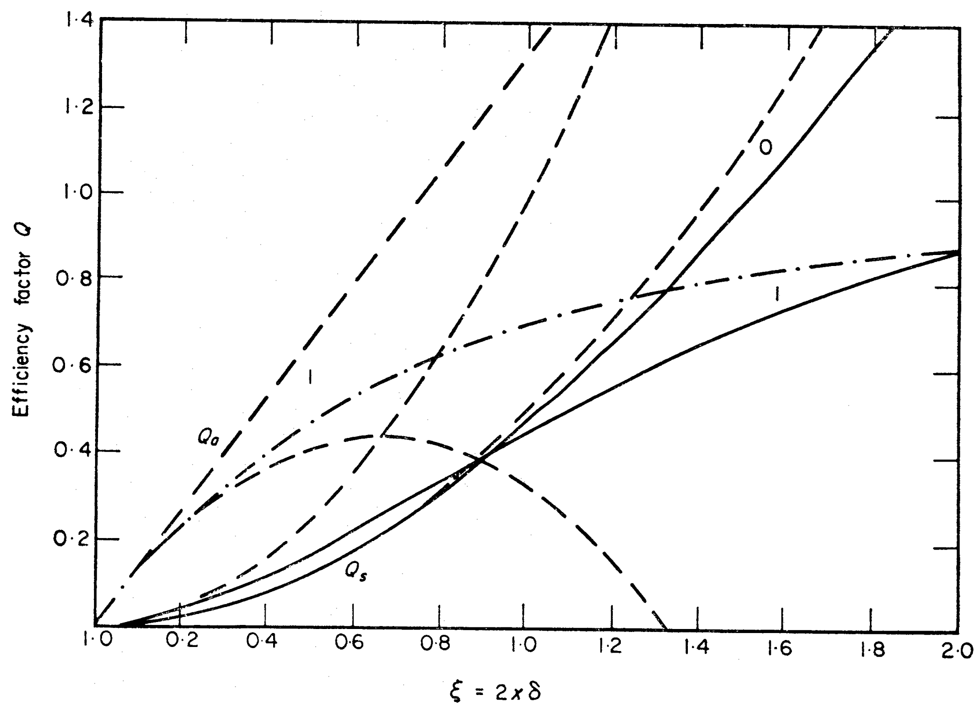

FIG. 1. *Rayleigh–Gans approximations (dashed curves) to the exact efficiency factors Q_s (solid curves) and Q_a (dash–dot curve) for homogeneous spheres with tan ϵ = 0 and 1 (curves 0 and 1 respectively).*

depends only on the shape of the geometrical shadow. However cFd will only be important in the extreme of very large grains and short wavelengths. Third, the effect of the transmitted radiation which is present when the grain is not opaque is seen to enter through the second term in the curly brackets. This transmitted radiation can interfere with the radiation outside the geometrical shadow, thus enhancing or decreasing the amount of extinction. The presence of an imaginary term in $m-1$ reduces the transmitted component, thus diminishing the interference effects (Fig. 1). In general the geometrical shadow is not uniformly illuminated so that the intensity distribution is different than that from an opaque grain (cFd). This has led to the name anomalous diffraction (van de Hulst).

One limiting case of interest occurs when the phase shift across the particle is small. In this case the first factor in the integrand reduces to

$$i\frac{2\pi}{\lambda}(m-1)\,p$$

and so $Q_s \propto |m-1|^2$. The introduction of absorption is seen to increase the scattered intensity without altering the angular distribution. This increase may be attributed to a reduction in the destructive interference between the transmitted and exterior radiation fields but more often (see next paragraph) is thought of as arising from an enhanced polarizability of the grain material.

This limiting case ($|\xi^*|$ small) of anomalous diffraction corresponds to a limiting case (x large) of Rayleigh–Gans scattering (RGs). Since RGs is most often used to describe X-ray extinction we give an alternate formulation which clarifies its limitations. Each small volume element is assumed to act independently as a source of Rayleigh scattering, the final amplitude being the coherent sum of the contributions from each small volume element. When x is large the radiation is confined to a narrow cone about the forward direction by interference effects. The theory is only valid when $|\xi^*|$ is small. Since $|m-1|$ is small, then $|\xi^*|$ may be sufficiently small even for large values of x. Examples of the departures from RGs for larger values of $|\xi^*|$ are given in Fig. 1 and in Section 4.

The efficiency factors for scattering and total extinction may be obtained in two ways, the method chosen depending on the ease of computation. The intensity of the scattered wave may be integrated over all solid angles giving

$$Q_s = \left(\frac{\lambda}{2\pi}\right)^2 \iint |S(\theta, \varphi)|^2 \, d\omega/G.$$

Having determined Q_a previously, we find $Q_e = Q_s + Q_a$. Or by determination of the intensity in the forward direction (amplitudes added) we find

$$Q_e = 4\pi\left(\frac{\lambda}{2\pi}\right)^2 \text{Real}\,[S(0)]/G.$$

TABLE I

Selected examples of efficiency factors and amplitude functions

Grain type: Shape	Grain type: Incident radiation	Rayleigh–Gans scattering: $Q_a < 1$	Rayleigh–Gans scattering: $Q_s < 1$	Rayleigh–Gans scattering: $S(\theta, \varphi)$	Classical Fraunhofer diffraction: $S(\theta, \varphi)$ ($Q_a = Q_s = 1$)
Sphere: radius a	—	$\frac{8}{3}x\beta$	$2x^2(\delta^2+\beta^2)$	$G(x\theta)$	$F(x\theta)$
Circular disc: radius a; thickness $2t$	Along axis	$4y\beta$*	$4y^2(\delta^2+\beta^2)$	$F(x\theta)$	$F(x\theta)$
Circular cylinder: radius a; length $2t$	Perpendicular to axis	$\pi x\beta$	$\frac{8}{3}x^2(\delta^2+\beta^2)$	$F(x\theta_x)\,E(y\theta_y)$†	$E(x\theta_x)\,E(y\theta_y)$

* $y = 2\pi t/\lambda$.
† $\theta_x = \theta \sin\varphi$; $\theta_y = \theta\cos\varphi$; $\varphi = 0$ on cylinder axis.

Some specific examples, calculated by van de Hulst, are given in Table I. The amplitude functions E, F and G are the Bessel functions of order $\frac{1}{2}$, 1 and 3/2 respectively, divided by the first term in their series expansion. They are quite similar but the lower order functions fall off more rapidly from the maximum of one at zero; half intensity points are 1·39, 1·61 and 1·81 respectively.

Guinier (1939) has pointed out that $G^2(u)$ (for a RGs sphere) is approximated quite closely by $e^{-u^2/5}$★. This is easily seen by studying the first few terms in the series expansions. Similarly $F^2(u) \sim e^{-u^2/4}$ and $E^2(u) \sim e^{-u^2/3}$, at least in the region where these functions are large. This approximation is useful for the calculations in Section 3.

The anomalous diffraction for a homogeneous sphere has been studied in detail (van de Hulst). To establish the values of $|\xi^*|$ at which the RGs is no longer valid we use (Section 4) the exact formulae

$$Q_a = 1 + \tfrac{1}{2}\{e^{-2\xi \tan \epsilon}[1 + 2\xi \tan \epsilon] - 1\}/(\xi \tan \epsilon)^2$$

$$Q_e = 2 - \frac{4 \cos \epsilon}{\xi}\left\{e^{-\xi \tan \epsilon}\left[\sin(\xi - \epsilon) + \frac{\cos \epsilon}{\xi}\cos(\xi - 2\epsilon)\right] - \frac{\cos \epsilon}{\xi}\cos 2\epsilon\right\} \qquad (1)$$

where $\tan \epsilon = \beta/\delta$ and $\xi = 2x\,\delta$. It is customary to display Q vs. ξ for fixed values of $\tan \epsilon$ (Fig. 1). This is useful to show some features of the theory we have discussed, and is also sufficient to show the effect of changing the grain size, or the wavelength when $\tan \epsilon = 0$. However, to study the wavelength dependence in realistic cases where $\tan \epsilon$ is a rapidly changing function no one curve (for fixed $\tan \epsilon$) is sufficient by itself, and the individual cases are best treated with the exact formulae (see Section 4).

We note in conclusion that in the extinction of X-rays the grains leave the initial polarization unchanged. This is due in part to $m-1$ being small and in part to x being large. Familiar results are that Rayleigh scattering (and hence RGs) shows no polarization dependence in the forward direction and similarly that cFd does not affect polarization. The fact that anisotropic shape does not introduce polarization can be seen, for example, from Greenberg's (1968) calculations for infinite cylinders.

3. THE X-RAY HALO

We now study the effects of interstellar grains on the X-rays from discrete sources. Each grain in the line of sight to the source reduces the X-ray intensity by absorption and scattering. The part that is truly absorbed is lost to the radiation field but the scattered radiation reappears in other directions. Consequently grains slightly displaced from the line of sight may be expected to scatter some of the radiation incident on them into a cone with apex at the observer. In fact a uniform screen of grains will replace all the radiation that is scattered from the line of sight, resulting in a halo around the source. As pointed out by Overbeck (1965) and later by Slysh (1969) this halo can in principle be observed since small angle scattering produces a correspondingly small halo. The total intensity of the halo is $1 - e^{-\tau_s}$ relative to a value $e^{-\tau_s}$ for the central source and both will be reduced equally by the factor $e^{-(\tau_a + \tau_g)}$ where τ_s, τ_a and τ_g are optical depths for scattering and absorption by the grains and absorption by the gas respectively.

★ Actually Guinier's approximation corresponds to the solution for an infinite sphere (RGs) in which the polarizability of the grain material (or density in the case of X-rays) decreases as $e^{-(r/a')^2}$ with radius r, a' being related to the radius a of the approximated sphere by $a'^2 = \frac{2}{5}a^2$. The increased radius and decreased polarizability have compensating effects.

We shall refer to the relative intensity $e^{\tau_s}-1$ in Section 4. A useful estimate of this intensity can be obtained by comparing the X-ray optical depth τ_s to that in the visual, τ_e. If the same grains are responsible for the extinction then

$$\tau_s = \tau_e Q_s / Q_e.$$

Using $Q_s \sim 0 \cdot 1$ (Section 4) and $Q_e \sim 2$ with $\tau_e \sim 2$ per kpc gives a relative intensity $\sim 0 \cdot 1$ for a source at one kiloparsec.

It is important that the angular intensity distribution in the halo arising from an optically thin screen of grains is of the same form as that from a single grain, except scaled down by the ratio r, the distance from the source to the grains expressed as a fraction of the total distance to the observer. The following discussion will revolve around the various factors which modify this initially simple distribution.

The size of the halo is a useful parameter when comparing observations to the predictions of a theory. The total intensity in the halo may be found from the integral

$$I \propto \int_0^\pi |H(\alpha)|^2 \alpha \, d\alpha.$$

(We have chosen an axially symmetric case with amplitude function $H(\alpha)$ where α is the angle to the line of sight measured at the observer, and for convenience $|H(0)| = 1$.) It is a peculiarity of functions H which can be approximated by $e^{-K\alpha^2}$, K being constant, that the fraction of radiation inside a cone of half angle α_c is $\sim 1 - |H(\alpha_c)|^2$. Thus the angle $\alpha_{c1/2}$ for a cone containing half the radiation is equal to the angle $\alpha_{1/2}$ at which $|H(\alpha)|^2$ reaches a value of one half. For an optically thin halo with single particle scattering function $F(\alpha)$ we find

$$\alpha_{1/2} \sim \frac{\lambda}{2a} 2r$$

minutes of arc when λ is measured in Ångstroms and a in units of 10^{-5} cm. This applies only to the scattered radiation; the unscattered radiation at $\alpha = 0$ must be subtracted. In practice, however, such simple considerations will likely not be sufficient and in general $\alpha_{c1/2} \neq \alpha_{1/2}$.

An important consequence of the single particle scattering is that particles of anisotropic shape could produce a non-circular halo if suitably aligned. Current theories of the polarization of starlight require anisotropic grains, aligned in some cases to a high degree which might produce an observable effect on the halo. The electric vector of the polarized light is perpendicular to the long axis of the grain, so that the halo should be elongated parallel to the observed electric vector. From such observations some estimate of the grain elongation and alignment could be obtained, giving a possible distinction between proposed grain models.

Factors such as the size distribution of the grains, the bandwidth of the detector, the position of the grains in space and multiple scattering tend to disguise the intensity distribution attributable to a single particle. It can be seen from the formula above for the halo size that changes in λ, r and $1/a$ have similar effects. It would be difficult to disentangle them in an observation but it is possible to describe each individually. This will help clarify the problems involved in estimating the grain size from the width of the halo.

The size distribution ($n(a)\,da$) is needed to determine the total intensity in the halo as well as the distribution across it. The contribution of a grain of radius a to τ_s is $C_s = \pi a^2 Q_s$ so that $\tau_s \propto a^4$ for RGs and $\tau_s \propto a^2$ for cFd. The dominant sizes are determined by the product $C_s n(a)$. For example, Greenberg's (1966) approximation to the Oort–van de Hulst distribution is $n(a) \sim \exp\,[-5(a/a_0)^3]$ for which, in the case of RGs, 75 per cent of τ_s arises from $0{\cdot}45 < a/a_0 < 0{\cdot}85$ with contributions from different sizes varying by less than a factor of two. Thus $C_s n(a) \sim$ constant is a good approximation for this range of grain sizes. We note that cFd favours smaller values of a/a_0. Only in the optically thin case is the halo intensity directly proportional to τ_s.

We illustrate the effect of a size distribution on the halo from RGs spheres of radii a_1 to fa_1 ($f > 1$) for which $n(a) \sim a^{-4}$. All sizes give equal contributions to the total but produce different angular distributions. Using Guinier's approximation to G^2 we find

$$I(\alpha) \sim \int_{a_1}^{fa_1} a^2 \exp\left[-\frac{1}{5}\left(\frac{2\pi\alpha}{\lambda r}\right)^2 a^2\right] da$$

which may be expressed in terms of the error integral or numerically integrated. The form of the integrand clearly shows that large grains dominate in the central part of the halo but contribute little at larger angles where small grains become important. In Fig. 2 $I(\alpha)$ is shown for $f = 3$ (curve f). This curve should be

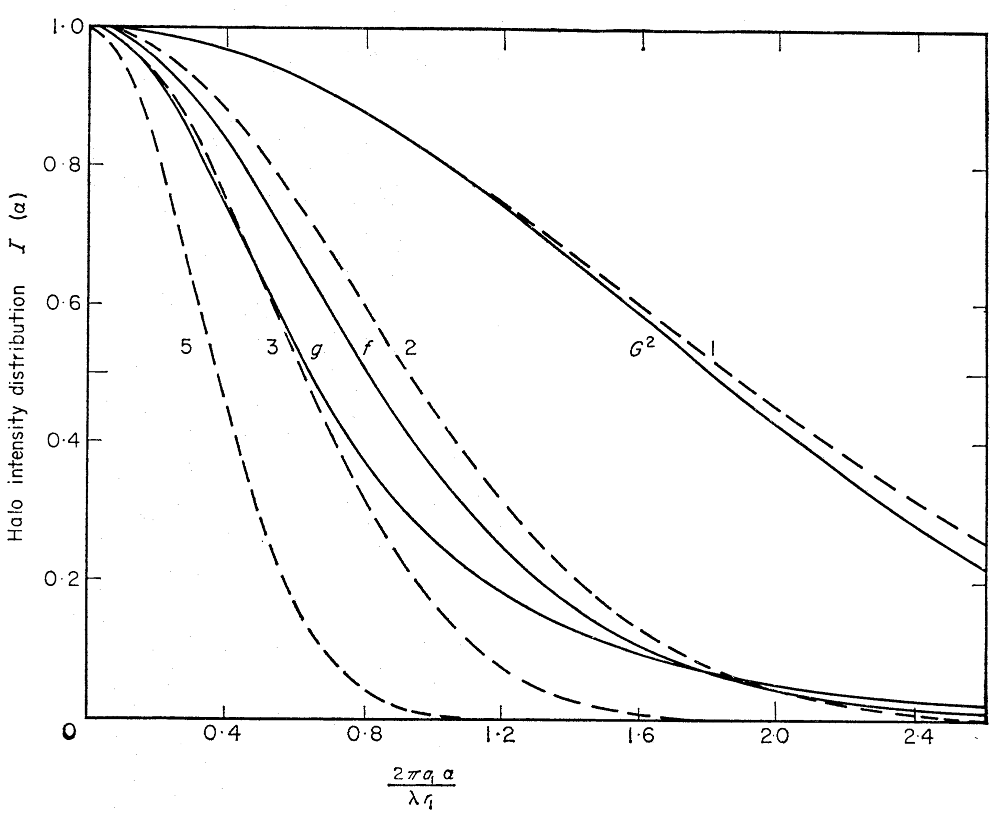

FIG. 2. *The intensity distribution of the halo from RGs homogeneous spheres for an optically thin medium. Curve G^2 is exact for $ar_1/a_1r = 1$ whereas curves 1, 2, 3 and 5 are Guinier's approximations for $ar_1/a_1r = 1$, 2, 3 and 5 respectively. A screen of grains at r_2 with size distribution $n(a) \sim a^{-4}$ from $a = a_1r_1/r_2$ to $3a_1r_1/r_2$ gives distribution f. Curve g arises from a uniform medium of grains of radius a_2 extending from $r = r_1a_2/a_1$ to $r_1a_2/5a_1$ ($r < 1$).*

compared to those marked 1, 2 and 3 which correspond to single particle sizes a_1, $2a_1$ and $3a_1$ respectively. The grain size giving the best approximation to $I(\alpha)$ at half intensity ($\alpha_{1/2}$) is $2 \cdot 2a_1$. In general, measurement of $\alpha_{1/2}$ favours the larger grains since it is the smaller grains that scatter radiation into the long tail. It is important to note that now $\alpha_{c1/2} > \alpha_{1/2}$; however $\alpha_{c1/2}$ is harder to measure unless the outer region of the halo is detectable.

A finite bandpass in the detector with response $D(\lambda)\, d\lambda$ causes a similar effect. The optically thin halo from RGs spheres has

$$I(\alpha) \sim \int D(\lambda)[\lambda^2 + d_1{}^2(\lambda)]\lambda^{-2} \exp\left[-\frac{1}{5}\left(\frac{2\pi a\alpha}{r}\right)^2 \frac{1}{\lambda^2}\right] d\lambda$$

where $d_1(\lambda)$ gives the wavelength dependence of the absorption coefficient of the grain material. This complication can be removed by the use of a sufficiently narrow bandpass. The observations suggested in the next section require good wavelength resolution for other reasons.

Multiple scattering can be very important. Dexter & Beeman (1949) have made an analytical study of the scattering of an X-ray beam by a uniform medium of spheres. They find that the component which has been scattered n times has a width $\sqrt{n}$ times that of the singly scattered component. The spreading of the halo may be thought of as the result of a random walk process perpendicular to the direction of the original beam. Dexter and Beeman also showed that the nth component has a significant effect when $\tau_s \sim n+2$. This is a useful estimate of the integrated result. For example, we may expect the singly scattered halo (optically thin) to be broadened by a factor $\sim \sqrt{3}$ when $\tau_s \sim 5$.

A qualitative description of the joint effect of multiple scattering and a size distribution can now be given. Since the contributions to τ_s from all grain sizes will not in general be equal, and since the amount of broadening due to multiple scattering has only been estimated the determination of the grain size could be quite confused. Accurate computations of the intensity distribution may be obtained from a Monte Carlo calculation if $n(a)$ and the optical depth τ_s (and the space distribution) are known. For example Overbeck (1965) has treated the case of a uniform medium of RGs spheres with $n(a) \sim e^{-\frac{1}{2}(a/a_0)^2}$ for several values of τ_s. In view of the uncertainty of $n(a)$ and the similarity in shape of Overbeck's results for different τ_s we accept curves such as f derived in the optically thin case to be suitable approximations if widened appropriately (as above) and the conclusions drawn from the optically thin case can then be carried over. The introduction of a finite bandpass with multiple scattering is similarly more complicated.

Next we examine the effect of the distribution of the grains in space. In general, grains situated close to the source produce smaller halos. Thus a source embedded in a 'cloud' of grains would have a smaller halo than it would have if a uniform medium existed between the source and the observer. Similarly extragalactic sources would have larger halos than galactic sources in the same direction if the distribution in the galaxy is fairly uniform. To study the integrated effect from grains at several distances we take a uniform medium extending from ratio r_1/g to r_1 ($g > 1$) which for RGs spheres gives

$$I(\alpha) \sim \int_{r_1/g}^{r_1} r^{-2} \exp\left[-\frac{1}{5}(x\alpha)^2 \frac{1}{r^2}\right] dr.$$

This integral may also be expressed in terms of the error integral or may be numerically integrated. The curve obtained for $g = 5$ is shown in Fig. 2 (curve g). It should be compared to those marked 1, 3 and 5 which correspond to single ratios r_1, $r_1/3$ and $r_1/5$ respectively. The half intensity point $\alpha_{1/2}$ corresponds to a ratio $r_1/3$ and again $\alpha_{c1/2} > \alpha_{1/2}$. The most distant grains (r small) are favoured if the outer part of the halo is not observed, since the long tail is produced by the grains closest to the observer. Multiple scattering may be taken into account by broadening curves such as g.

There is ample evidence that the material causing the interstellar extinction is not evenly spread out in space. On the contrary, many attempts have been made to explain the observations by what are tentatively called clouds. It is the small scale of the irregularity that is important to the following; the concept of spherical clouds has been used to facilitate the discussion.

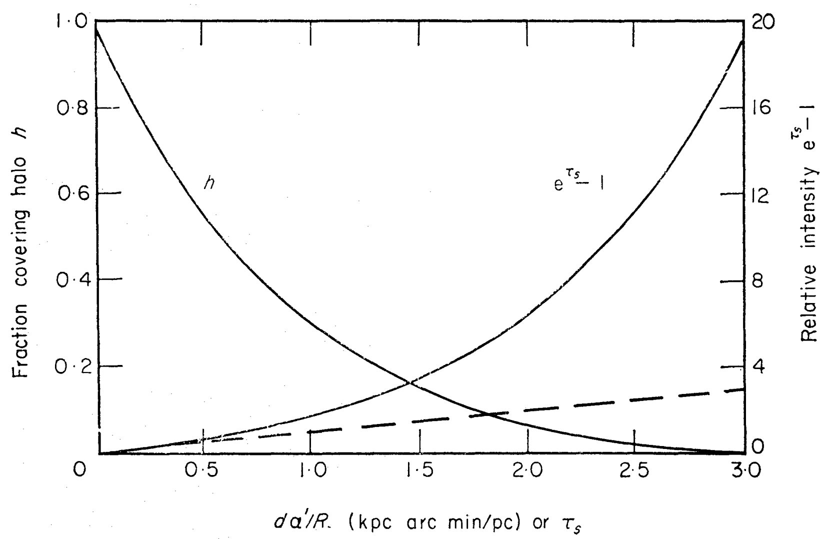

FIG. 3. *The fraction of intercepted clouds which cover the halo, curve h (Section 3). The intensity of the halo relative to the unscattered central source, with linear approximation for small τ_s (Section 4).*

One extreme example is a cloud of grains slightly displaced from the line of sight. The line of sight observations would not be affected, so that any scattered radiation would actually increase the total received. On one side of the source would be a halo, depending on the cloud's shape, density and distance as well as its displacement from the line of sight. In a more general situation we should not expect that the line of sight passes through the centre of each cloud it encounters. Nor will each cloud cover the halo completely. The generators of a cone of half angle α_c will intercept $\pi R^2(1+\cos\theta)^2 n_c \Delta d$ clouds of radius R in a distance Δd, where $\cos\theta = \alpha_c d/R$, d is the distance to the clouds and n_c is the space density of the clouds. However only a fraction $h = [(1-\cos\theta)/(1+\cos\theta)]^2$ of these will cover the whole halo of size $2\alpha_c$. Furthermore, to ensure that the path length through any cloud is at least R, the effective radius $\sqrt{3}\,R/2$ should be used to determine d. Since all clouds affect some part of the halo, a low value of h can be taken to indicate some irregularity in the halo. Fig. 3 shows the variation of h with $d\alpha'/R$ where d is measured in kpc, α' in minutes of arc and R in pc. For $R = 7$ (Spitzer 1968) and $\alpha' = 7$, clouds at distances greater than 0·5 kpc should cause a measurable effect. We cannot expect a statistical averaging to take place as there are only eight such clouds per kpc in a line of sight.

When the factors discussed above are taken into account in the interpretation of the observations of an X-ray halo around a discrete source useful estimates of the grain size, shape and position in space can be obtained.

4. CHEMICAL IDENTIFICATION FROM ANOMALOUS SCATTERING

It has been pointed out in a previous paper (Martin & Sciama 1970) that if elements such as C, O, Mg and Si are prominent constituents of the interstellar grains their presence might be confirmed by high resolution studies of strong X-ray sources. The reason is that the spectrum of the halo would change in a characteristic fashion for X-ray energies near the K absorption edge of the relevant element in the grain, owing to the effect of anomalous dispersion.

In applying the dispersion theory for soft X-rays (Parratt & Hempstead 1954; Henke 1961) it was found convenient to express

$$\delta = A\lambda^2 \sum_j g_j \delta_j' \text{ and } \beta = A\lambda^2 \sum_j g_j \beta_j'$$

where g_j is the oscillator strength of the jth resonance, δ_j' and β_j' arise from a j-type electron, and $A = 2{\cdot}70 \times 10^{10}\, \rho/M$ (cgs). Furthermore it was shown that

$$\delta_K' = 1 - \frac{7}{8} d^7 \left\{ \ln \left| \frac{1+d}{1-d} \right| + \ln \frac{1+\sqrt{2}\, d + d^2}{1-\sqrt{2}\, d+d^2} + 2 \tan^{-1} d + \sqrt{2} \tan^{-1} \frac{\sqrt{2}\, d}{1-d^2} - K \right\}$$

where $d = y^{1/4}$, $y = \lambda/\lambda_K$ and the constant $K = \pi \cot(\pi/8)$ for $y < 1$ and $K = \pi$ for $y > 1$. Also $\beta_K' = (7\pi/8)\, y^{7/4}$ for $y < 1$ and $\beta_K' = 0$ for $y > 1$.

In this paper we wish to examine some of the assumptions underlying the initial analysis. First, it was assumed that the anomalous effect of the L electrons could be ignored since only energies close to the K edge were being considered. This remains a valid assumption. The absorption below the K edge was previously set equal to zero. Here we introduce an extra term in the absorption

$$\beta = 0{\cdot}35\, A\lambda^2 y^{1{\cdot}6}$$

which corresponds to about 7 per cent of the contribution β_K at $y = 1$. This can be taken to represent either L shell absorption or the background absorption by other elements in the grain. Clearly this is only an estimate chosen to illustrate the effect; it should be suitable for the example we discuss later. The major assumption however was that RGs was valid throughout the energy range examined. In some cases it appeared that this was marginal. Therefore we have examined the phenomenon by means of the exact formulae (equation (1)) so that a comparison could be made with the RGs approximation.

As a specific example, oxygen in (pure) ice grains was chosen ($\lambda_K = 23{\cdot}3$ Å, $\rho = 0{\cdot}91$ g cm^{-3}). Several grain sizes ($a = 0{\cdot}8$, 2 and 5×10^{-5} cm) were studied. For the first choice it was found that RGs was a good approximation, as expected. Graphical results for the larger grains are shown in Figs 4(a) and (b). Several comments can be made concerning these figures. Essentially what is being displayed is the anomalous behaviour of Q_s near the K edge (lower curves) in contrast to Q_s obtained from similar grains without the K absorption (upper curves). The dashed curves are from the RGs approximation whereas the solid ones are based on the exact equations. It is evident that the shape of the anomalous behaviour for RGs is independent of a. However, this is not true for the exact calculations where larger departures are seen to occur for larger a. This results from the

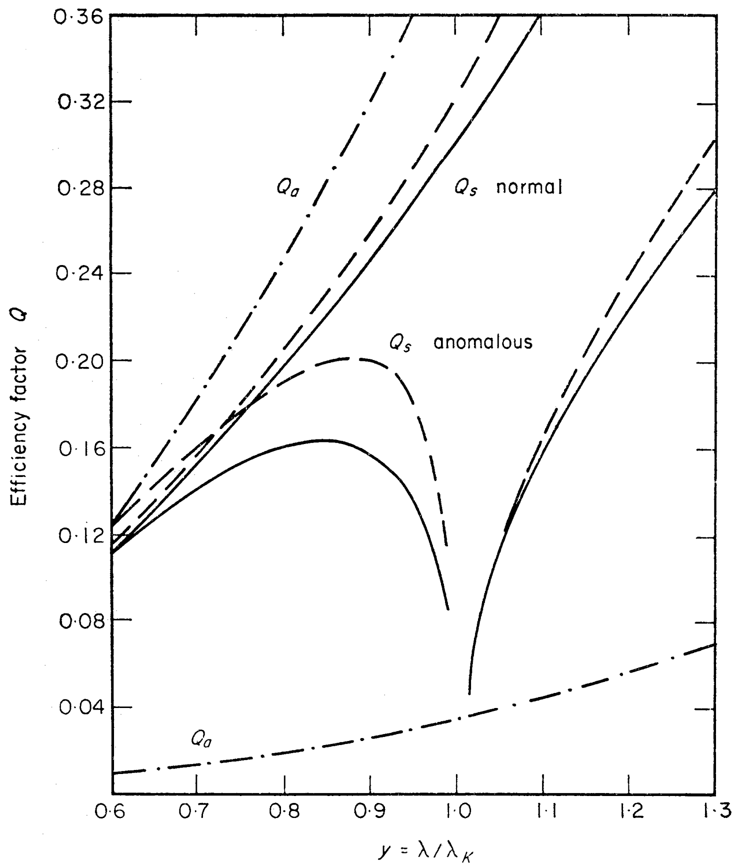

FIG. 4(*a*). *The anomalous behaviour of Q_s near the K edge of oxygen in ice grains of radius 2×10^{-5} cm (lower curves) compared to the normal behaviour in the absence of the K edge (upper curves). The dashed curves are the RGs approximation; solid curves are exact. The variation of Q_a is shown by the dash–dot curves.*

increased value of ξ, on which $|\xi^*|$ depends. The presence of the K absorption gives a high value of tan ϵ, thus also increasing $|\xi^*|$. Although some departures from the RGs approximation are possible, the anomalous behaviour of Q_s remains quite similar. It was found that the additional absorption we included had only a small effect. The dotted curve in Fig. 4(b) is the exact result without the extra absorption which was included in the calculations for all other curves.

Also shown in Fig. 4 are exact values of Q_a (dash–dot curves). The absorption optical depth τ_a due to grains is proportional to Q_a; this will affect the total intensity received from the source, but not the relative intensity of the halo to the central unscattered source, $e^{\tau_s}-1$, shown in Fig. 3. Only for small τ_s is the dependence of the relative intensity on Q_s linear; for larger values of τ_s the change is much more rapid. Account must be taken of this when reducing the observations.

We reach the same conclusion that by interpreting the spectrum of the halo of a source in terms of the anomalous scattering of X-rays near a K edge one might obtain convincing evidence on the composition of the grains.

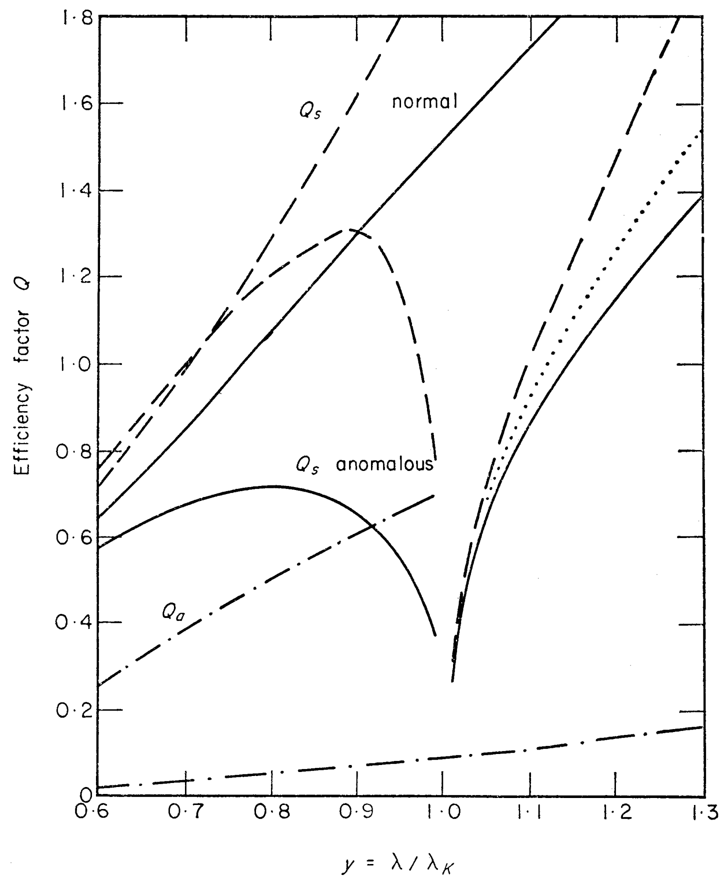

FIG. 4(*b*). *Same as Fig.* 4(*a*) *except that radius is* 5×10^{-5} *cm. The dotted curve shows the exact calculation for* Q_s *without the additional absorption that gives the lower curve for* Q_a.

5. CHEMICAL IDENTIFICATION BY ABSORPTION MEASUREMENTS

There is some possibility that chemical identification may be obtained from measurements of the absorption caused by grains. In general the grains will produce a K-edge phenomenon similar to that which would appear from atoms of the same element in the gaseous state. However, for a given amount of the element the absorption by grains could be less than that from the gas if the grains were large enough to be no longer optically thin. This could lead to underestimates in interstellar abundance determinations based on X-ray absorption observations.

In principle the fact that the element is in a grain may be revealed by more detailed observations. In a solid the wavelength of the K-edge shifts due to chemical combination and the potential field of neighbouring atoms. However this shift is small, in the range 1–10 eV, so that precise energy resolution would be required once the edge was identified. The more favourable opportunities would occur for the lighter elements with lower K-edge energies. There is also some possibility this might be confused by the K-edge absorption by ionized gases in thermal sources (Tarter, Tucker & Salpeter 1969), by elements combined in molecules (e.g. Chun 1969) or by the Kossel fine structure near the edge.

A more convincing but perhaps more difficult test would be the observation of the extended Kronig fine structure, a characteristic of the absorption by elements in solids. It may be described as an undulation in the absorption coefficient out to several hundred electron volts above the edge, with peak to peak spacings ~ 50 eV and amplitudes (q) approximately one tenth (at room temperature) of the discontinuity at the edge. This oscillation arises from the influence of neighbouring atoms on the density of states for the photoelectron as well as the transition probabilities to these states. Only within ~ 20 eV of the edge is there a chance of confusion with the Kossel fine structure which appears also for atoms and molecules. Azároff (1963) has given an extensive discussion of the theory in a review paper. We note only two later developments which have some relevance to interstellar grains. First, the fine structure has been observed for non-crystalline as well as crystalline solids (e.g. White & McKinstry 1966) in agreement with the theory of Kozlenkov (1963) and Shmidt (1963). This takes on some importance as the degree of order in interstellar grains is not well understood. The Kozlenkov–Shmidt theory has predicted that the amplitude of the fine structure should increase as the temperature is lowered and the experiments of Boster & Edwards (1968) apparently confirm this. Thus values of $q \sim 0{\cdot}25$ might be expected in the temperature range 3°–30°K.

For the remainder we take a pragmatic interest in this phenomenon, representing it by a change $\Delta\tau$ in the average optical depth τ_2 of the edge. The quantity τ_2 arises from the K absorption of the element concerned (gas and solid) added to the background absorption τ_1 of the gas (due in large part to H and He at low energies). If a fraction z of the K absorption is from elements in grains, then the intensity change in the feature is $e^{\Delta\tau} \sim 1 + qz(\tau_2 - \tau_1)$. In order to calculate $\tau_2 - \tau_1$ the relative abundances of the absorbing elements must be known, as well as the density in the line of sight. Brown & Gould (1969) have given τ in terms of n_H, the number of hydrogen atoms in the line of sight (the presence of elements in grains and therefore the possible scattering have been ignored). With their values of τ and an estimate $qz \sim 0{\cdot}1$ we have calculated $n_H(10)$, the line of sight hydrogen density required to produce a 10 per cent change in intensity ($\tau_2 - \tau_1 = 1$ in this case). In a medium with one atom of hydrogen per cubic centimetre there is a contribution of 3×10^{21} cm^{-2} to n_H every kpc. Thus the values for the lighter elements shown in Table II are not unreasonable. However it is also important that τ_2 is not so large that the source is undetectable. We have calculated $\tau_2(10)$ and $\tau_2'(10)$ (corresponding to $n_H(10)$) for energies at the

TABLE II

Parameters for fine structure

	$n_H(10)$ (cm^{-2})	E_K (keV)	$\tau_2(10)$	$\tau_2'(10)$
C	$2{\cdot}3 \times 10^{21}$	0·28	6·9	2·8
N	9·5	0·40	11·0	5·5
O	1·7	0·53	1·8	1·1
Mg	180	1·3	19·0	15·0
Si	210	1·8	8·6	7·3
S	290×10^{21}	2·5	6·5	5·7

edge and 100 eV above it respectively. Close to the edge the H–He contribution to τ_2 is largest and somewhat diminishes the favourable effect of the high relative abundances of the lighter elements. Some attention should be paid to the possibility of overlapping of C–N–O fine structures. We note that this method of chemical identification is in a way complementary to that of Section 4 since here large optical depths are needed.

The following considerations are important in the evaluation of observational possibilities. The value qz could be as large as 0·3, reducing our estimates of $n_{\mathrm{H}}(10)$ and $\tau_2(10)$ by a factor of three and thereby substantially improving the prospects of such observations. A similarly more favourable situation would exist if the threshold for detection of the fine structure could be lowered. More important is the fact that the spectra of X-ray sources (with the exception of some thermal sources) continue to rise at the low energies which are required. Moreover there is evidence for sources which are very bright at low energies (Grader *et al.* 1969); such sources could prove to be very useful. One major difficulty might be source variability in times comparable to the (long) integration time.

The diffuse X-ray background (Oda & Matsuoka 1969) might also be used to measure the fine structure since suitably large optical depths would occur. Radiation could be accepted from advantageously large solid angles as long as this was compatible with the method of energy resolution.

We conclude that this fine structure might be observed for the lighter elements, especially C and O. Any attempted observations should be restricted to those sources (or directions) which show a sufficient jump in optical depth at the K edge. These could be obtained from a preliminary list of K edges since such documentation would no doubt be available before this experiment was performed.

ACKNOWLEDGMENTS

I would like to thank Dr D. W. Sciama for his interest in initiating this investigation and his encouragement throughout its development. I am indebted to the Association of Commonwealth Universities for the award of a Commonwealth Scholarship.

Department of Applied Mathematics and Theoretical Physics, University of Cambridge.

REFERENCES

Azároff, L. V., 1963. *Rev. mod. Phys.*, **35**, 1012.
Brown, R. L. & Gould, R. J., 1969. Submitted to *Astrophys. J.*
Boster, T. A. & Edwards, J. E., 1968. *Phys. Rev.*, **170**, 12.
Chun, H. Y., 1969. *Phys. Lett.*, **30A**, 445.
Dexter, D. L. & Beeman, W. W., 1949. *Phys. Rev.*, **76**, 1782.
Grader, R. J., Hill, R. W., Seward, F. D. & Hiltner, W. A., 1970. *Astrophys. J.*, **159**, 201.
Greenberg, J. M., 1966. I.A.U. Symposium No. 24, '*Spectral Classification and Multicolour Photometry*', p. 291, eds K. Lodén, L. O. Lodén and U. Sinnerstad, Academic Press, London.
Greenberg, J. M., 1968. *Stars and Stellar Systems*, *Vol.* 7, p. 221, eds B. M. Middlehurst and L. H. Aller, University of Chicago Press.
Guinier, A., 1939, *Ann. Phys.*, *Paris*, **12**, 161.

Henke, B. L., 1961. *Adv. X-ray Anal.*, **4**, 244.
Hulst, H. C. van de, 1957. *Light Scattering by Small Particles*, John Wiley and Sons, New York.
Kozlenkov, A. I., 1963. *Izv. Akad. Nauk SSSR Ser. fiz.*, **27**, 364.
Martin, P. G. & Sciama, D. W., 1970. *Astrophys. Lett.*, **5**, 193.
Oda, M. & Matsuoka, M., 1969. Cosmic X-rays, manuscript for Progress in Cosmic Ray Physics, ed. J. G. Wilson.
Overbeck, J. W., 1965. *Astrophys. J.*, **141**, 864.
Parratt, L. G. & Hempstead, C. F., 1954. *Phys. Rev.*, **94**, 1593.
Shmidt, V. V., 1963. *Izv. Akad. Nauk SSSR Ser. fiz.*, **27**, 384.
Slysh, V. I., 1969. *Nature*, **224**, 159.
Spitzer, L., Jr., 1968. *Diffuse Matter in Space*, Interscience Publishers, New York.
Tarter, C. B., Tucker, W. H. & Salpeter, E. E., 1969. *Astrophys. J.*, **156**, 943.
White, E. W. & McKinstry, H. A., 1966. *Adv. X-ray Anal.*, **9**, 376.